Anal Bioanal Chem (2009) 393:1571–1578
DOI 10.1007/s00216-008-2499-5

REVIEW

Portable Raman explosives detection

David S. Moore · R. Jason Scharff

Received: 1 October 2008 / Revised: 22 October 2008 / Accepted: 23 October 2008 / Published online: 21 November 2008

Abstract Recent advances in portable Raman instruments have dramatically increased their application to emergency response and forensics, as well as homeland defense. This paper reviews the relevant attributes and disadvantages of portable Raman spectroscopy, both essentially and instrumentally, to the task of explosives detection in the field.

Keywords Raman spectroscopy · Field analysis · Fluorescence interference · Explosives detection

Introduction

As the number and sophistication of terrorists increase, so too must the populace and their defenders continually improve and increase means for their detection and mitigation. In one small corner of that universe exist spectroscopic methods for detection of the harmful substances terrorists use, mainly because of spectroscopy's capacity for high selectivity and sensitivity [1–3]. One of these methods that has recently seen a dramatic increase in use is portable Raman spectroscopy, a vibrational spectroscopic method. It has been more than 5 years since the last reports on portable Raman spectroscopy for field detection of explosives [4–6], and there have been recent dramatic advances in portable Raman devices. This review strives to bring the field up to date.

Dedicated to Prof. Günter Gauglitz on the occasion of his 65th birthday.

D. S. Moore (✉) · R. J. Scharff
Shock and Detonation Physics Group,
Los Alamos National Laboratory,
Los Alamos, NM 87545, USA
e-mail: moored@lanl.gov

Vibrational spectroscopy is capable of the unique identification of molecular substances [7]. This capability exists because of each molecule's unique vibrational frequencies, which depend on the details of the molecular structure—bond lengths, bond strengths, and masses—and the coupling of these molecular motions to light. Infrared absorption occurs when an infrared photon incident on the molecule has a frequency resonant with that of one of the molecular motions. The absorption strength depends on the change in dipole moment that occurs during the molecular motion. The infrared absorption vibrational spectrum is then obtained by scanning the infrared frequency while recording the absorption. Alternatively, Fourier transform methods can be used in which a broad range of infrared frequencies are simultaneously incident on the molecules located in one arm of an interferometer, and the frequency spectrum is obtained by Fourier transform of the interferogram.

Raman scattering is another method for obtaining the vibrational spectrum of molecules [7, 8]. Some of the light incident on a molecule is scattered. The overwhelming majority of the scattering is elastic (incident and scattered wavelengths are the same), known as Rayleigh scattering. A small fraction of the scattering (approximately 10^{-7}–10^{-8}) occurs via an inelastic scattering process (incident and scattered wavelengths are different) known as Raman scattering. The energy difference between the incident and scattered photons is equal to the vibrational energy of a molecule or crystal and/or the rotational energy of a molecule. The inelastic scattering from a molecule or crystal in its rotational or vibrational ground state produces the Stokes Raman spectrum, a redshifted spectrum. The inelastic scattering from a molecule in a vibrational (or rotational) excited state may produce a blueshifted Raman spectrum, the anti-Stokes Raman spectrum. The relative intensity of the Raman lines in the Stokes and anti-Stokes Raman spectra

may be employed, using the Boltzmann equation, for the determination of the vibrational (or rotational) temperature. The strength of a Raman transition is determined by the change in molecular polarizability; molecular vibrational symmetries that modulate the molecular polarizability are Raman active, others are not. Raman spectra can be obtained using Fourier transform techniques, wherein the scattered light is collected and routed into an interferometer. Alternatively, dispersive methods using high-throughput spectrometers and very sensitive multichannel detectors are used. All of the portable Raman instruments discussed in this review are of this latter type.

The detailed theory of the Raman process is available elsewhere [7–10]. For our discussion of portable Raman instruments, we will only utilize the details about Raman signal strength for the 180° backscattering arrangement (used in the devices discussed here), its excitation wavelength dependence, and the effects of absorption and scattering in the sample. We will also discuss the specific instrumental factors that affect accuracy of the spectra, i.e., abscissa (Raman shift axis) calibration and ordinate (intensity axis) correction.

Raman spectroscopy as a tool to detect hazardous substances in the field is attractive also because little or no sample preparation is necessary, it can be used through glass walls (such as vials) and through transparent plastic and thin translucent materials (such as bags and envelopes), the process (for the most part unless the sample is highly absorbing—see later) is noninvasive and nondestructive, and very small samples sizes can be used. Examples of each of these abilities are illustrated herein.

Instrumentation

Present portable Raman instruments can be represented schematically as in Fig. 1. The essential parts are a laser; an optics block containing a bandpass filter to pass just the laser wavelength, a dichroic mirror to pass the laser wavelength and reflect longer wavelengths (for Stokes Raman devices as discussed here), a lens to focus the laser onto the sample and collect the Raman scattered light, and a long wavelength pass filter to block residual reflected or scattered laser wavelength light; a spectrometer to disperse the Raman spectrum; and a multichannel detector such as a CCD. The mirror in the optics block is used for compactness, but is not essential to operation. Some kind of computer system is needed to operate the laser and collect and analyze the spectrum from the CCD.

There are a number of manufacturers of portable Raman instruments at the present time (Table 1). With one exception, they all utilize a diode laser as the excitation source. The exception uses a 532 nm frequency-doubled diode-pumped solid-state Nd:YAG laser. The 785 nm diode laser is most common, although 830 nm and other wavelengths have been used (however none of the instruments in Table 1 utilize them).

The instruments in Table 1 cover both portable and hand-held devices, the difference being plug powered versus battery powered and self-contained, respectively. They also cover both direct (free space) optics probes and optical-fiber-coupled probes. In Fig. 1, the optical fiber coupled probe devices are illustrated by adding optical fiber couplings between the optics block and the laser and the spectrometer, as shown in the dashed block.

The relevant differences between free-space-optics and optical-fiber-coupled probes are the laser power at the focus, the size of the focal/signal generation region, and the optical conductance from the sample through the spectrometer to the detector. Free-space optics serve to transform the Gaussian (assuming it is Gaussian) output of the excitation laser into a Gaussian focal region. Fiber coupling results in a larger focal volume because the end of the optical fiber is imaged; the fiber diameter in these instruments is on the order of 0.1 mm. The depth of focus is also larger than that of the free-space-optics systems. However, the number of excitation photons is determined by the power of the laser in each case. As long as the Raman process is not saturated, the Raman intensity is proportional to the excitation intensity. More exactly [7, 8], the radiance of a Raman line (scattered power per unit solid angle per unit area of sample integrated over the Raman

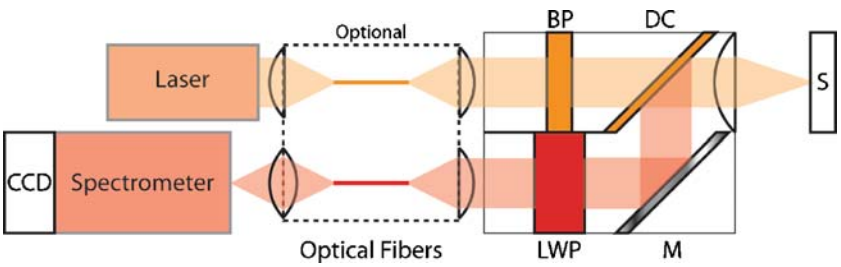

Fig. 1 Essential elements of a portable Raman system. *CCD* charge coupled device detector, *BP* bandpass filter, *DC* dichroic filter, *LWP* long wavelength pass filter, *M* mirror, *S* sample; optional optical fiber coupling shown in the *dashed block*

line) is equal to the radiant power Φ_0 of the exciting radiation divided by the cross-sectional beam area $r^2\pi$ and multiplied by the Raman scattering coefficient s_R:

$$L_R = \frac{\Phi_0}{r^2\pi} d\, s_R, \quad (1)$$

where d is the thickness of the observed sample volume and r is the beam radius [8]. For a given molecule and concentration, the signal at the detector is then determined by the optical conductance of the detection and dispersion system [7, 8]:

$$\Phi_{det} = LG\tau, \quad (2)$$

where Φ_{det} is the detected radiant power, L is the radiance of the Raman line, G is the optical conductance, and τ is the transmission factor of the system. For example, the optical conductance of an area F radiating into a solid angle Ω is

$$G_F = n^2 F \Omega. \quad (3)$$

Assuming we are working in the atmosphere so that the index of refraction $n \sim 1.0$, we can approximate the optical conductance of a system with areas F_1 and F_2 separated by a distance f_{12} (if the areas are much smaller than the separation distance) by

$$G \sim F_1 F_2 / f_{12}^2. \quad (4)$$

For the Raman radiance source described above, Eqs. 1, 2, 3, and 4 then provide the signal at the collecting lens Φ_{coll} (with collection angle Θ):

$$\Phi_{coll} = 4\pi\Phi_0 d s_R \sin^2(\Theta/2), \quad (5)$$

which does not depend on the area of the Raman radiant source (small-source approximation). Thus, the collected signal will be equal for all these Raman systems, given equal collection lenses and laser wavelength and power—see below.

In a correctly designed optical instrument, each imaging element produces an image of the preceding imaging element upon the following one. On all successive elements, the images of the first two elements (e.g., the source and the collecting lens) alternate. For such an instrument, the optical conductance between any two apertures in a sequence is invariant; therefore, the radiance observed at any cross section of the beam of an optical instrument is invariant. The optical conductance of the part of the arrangement that, for theoretical or technical reasons, cannot be enlarged determines the effective optical conductance of the entire instrument [7]. In the case of these Raman instruments, this limiting aperture is the spectrometer slit and/or the optical fiber.

Assuming that the numerical aperture of the collecting lens and the transmission factor are the same in each portable Raman instrument (for illustration purposes), then the only difference in their capabilities for conducting the Raman intensity to the detector is the optical conductance through the spectrometer slit. For the free-space-optics instruments, the diameter of the Raman radiating area is usually smaller than the spectrometer slit, so the radiating area is the limiting aperture. However, for the fiber-coupled instruments, the diameter of the Raman radiating area is typically larger than the spectrometer slit width, so the slit is the limiting aperture. To illustrate this, a 100-μm-diameter optical fiber is posited to carry the exciting laser light to the filtered probe optics. The end of the optical fiber is focused with unit magnification onto the sample. The Raman radiance is collected using the same lens and filtered before being focused, again at unit magnification, into the collection fiber, which is in turn focused at unit magnification onto the spectrometer slit. The ratio of the optical conductance of the radiant source to that of the spectrometer slit is $\pi r^2/sh$, where r is the radius of the radiant area and s and h are the slit width and height, respectively. We can

Table 1 Presently available portable Raman systems suitable for field use (not intended to be exhaustive)

Manufacturer	Product	Laser	Probe	Comments
Ahura Scientific [11]	First Defender	785 nm diode	Direct or Fiber	Self-contained
B&W Tek [12]	MiniRam II	785 nm diode	Fiber	GRAMS
DeltaNu [13]	Inspector Raman	785 nm diode	Direct	Laptop
DeltaNu	ReporteR	785 nm diode	Direct	Self-contained
Enwave Optronics [14]	EZRaman	785 nm diode	Direct	High-performance and low-cost versions
InPhotonics [15]	InPhotote	785 nm diode	Fiber	Laptop
Ocean Optics [16]	R-3000	785 nm diode	Fiber	Laptop
PerkinElmer [17]	Raman Identicheck	785 nm diode	Fiber	Steel encased fiber probe
Raman Systems [18]	RSL plus	785 nm diode	Fiber	Laptop or ultracompact
Renishaw [19]	RX210	785 nm diode	Fiber	
Senspex [20]	Ram-On	532 nm diode-pumped solid-state	Fiber	Self-contained
Smiths Detection [21]	RespondeR RCI	785 nm diode	Direct	Self-contained

model the ratio of optical conductance of an optical fiber to that of the intersectional area of a slit and an optical fiber as a function of the fiber radius as in Fig. 2. For fiber diameters greater than the slit width, the slit limits the optical conductance of the system. For a typical fiber diameter of 100 μm and a slit width of 10 μm (chosen to match a CCD pixel width) the optical conductance ratio is 7.85. For the free-space-optics instrument (or a fiber whose diameter is 10 μm), the optical conductance ratio is 1.0. This means a free space optics based instrument, all else being equal, can transmit significantly more Raman radiant power to the detector than an optical-fiber-coupled instrument. The slit width was chosen in the above example to match the detector pixel width to maximize the spectrometer resolution. Many instruments use larger slit widths to increase the optical conductance, which, however, degrades the resolution. This compromise provides the incentive to utilize free-space optics instead of optical-fiber coupling. For versatility in accessing samples, however, optical-fiber-coupled probes are often necessary. A method to partially circumvent this compromise is to utilize a circular fiber bundle at the probe and transition to a linear array aligned along the slit, as illustrated on the left side of Fig. 2.

Detector and laser considerations

Si-based CCD detectors

Si-based CCD detector technology has advanced considerably in recent years. The quantum efficiencies obtainable using backside-illuminated and thinned detectors along with antireflection coatings can be as high as 95% at the peak, a gain of nearly a factor of 2 versus front-illumination open-electrode CCDs.

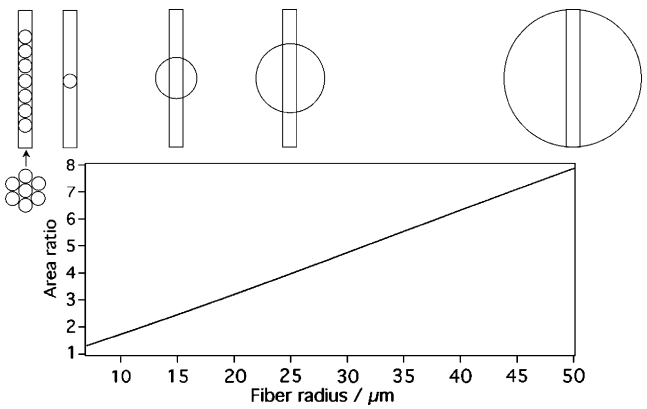

Fig. 2 The loss in optical conductance at a spectrometer slit for various optical fiber radii. The slit is 10 μm wide and 100 μm high. The ratio is the fiber circular area to the intersectional area of the fiber and the slit. Each of the four drawings is located vertically over its respective fiber radius. A circular to linear fiber bundle assembly (six-around-one to seven-in-a-line) to alleviate part of the loss without degrading spectrometer resolution is illustrated at the *far left*

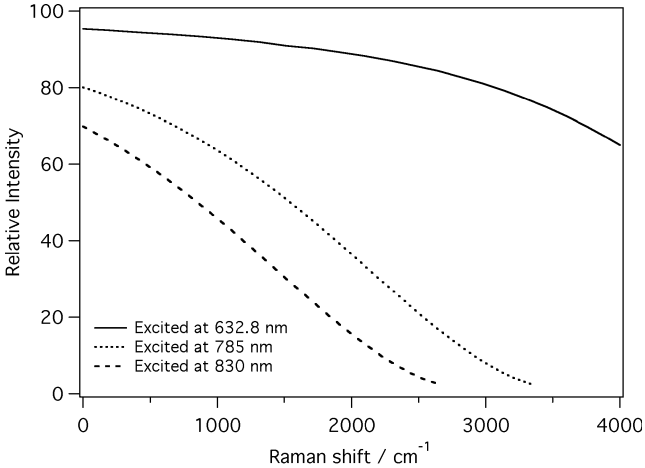

Fig. 3 Relative Raman intensity for Si-based CCD detectors for three different excitation wavelengths, based on a quantum efficiency versus wavelength curve for a thinned, backside-illuminated, visible antireflection coated CCD

Many authors and portable Raman instrument manufacturers comment on the Raman spectral wavenumber range available using various excitation wavelengths and Si-based CCDs, and make statements such as with Si-based CCD detectors and 785-nm excitation, Raman data can be accumulated out to more than 3,250-cm^{-1} Raman shift (including the CH stretch region), whereas Raman spectra obtained using 830 nm diode lasers cut off above 2,200 cm^{-1}. However, such statements can be misleading, as shown in Fig. 3. To obtain the plots in Fig. 3, a representative actual quantum efficiency curve for a common CCD camera (Andor DU420, thinned, back-illuminated, visible antireflection coating [22]) is plotted versus Raman shift wavenumber for three different excitation wavelengths, 632.8, 785, and 830 nm. Note that, while the cutoff wavelength commonly quoted is approximately 2,500 cm^{-1} for 830-nm excitation and approximately 3,250 cm^{-1} for 785-nm excitation, the sensitivity of the detector falls rapidly with wavelength through the entire Raman spectral region, so the features at larger Raman shift will suffer much more from noise than those at smaller Raman shifts. Even using 785-nm excitation, the detector sensitivity is more than a factor of 2 higher at 200 cm^{-1} than at 2,000 cm^{-1} and more than a factor of 10 higher than in the CH stretch region. Nevertheless, as most of the fingerprint region shown to be adequate to identify explosives lies between 200 and 2,000 cm^{-1}, the Si cutoff is not that important for systems based on 785 nm lasers [23].

Other detector materials

Both Ge- and InGaAs-based near-infrared (NIR) detector arrays have been investigated for use with longer-wave-

length excitation, such as 830 nm diodes or the 1,064 nm fundamental of the Nd:YAG laser [24]. However, at the present time, these NIR detector arrays are much less sensitive, noisier, and much more expensive than Si-based CCDs, so none are presently found in the listed (Table 1) portable Raman instruments intended for field use.

Lasers

For reasons of cost, weight, and fluorescence mitigation, most portable Raman instruments utilize diode lasers. One of the systems in Table 1 uses a diode-pumped solid-state intracavity frequency-doubled Nd-based laser (Senspex Ram-On) with excitation wavelength of 532 nm.

Often Raman spectra are accompanied by, or even obscured by, large baselines from fluorescence or thermal emission. For most situations, the longer the excitation wavelength, $\lambda=1/\nu$, the fewer interferences from fluorescence. However, the Raman scattering cross section varies as ν^4, so there is a severe signal intensity penalty incurred by using red or NIR excitation. For example, the ratio of Raman-scattering cross sections for a given molecule (with no resonance effects) for 532-nm excitation versus 785-nm excitation is nearly a factor of 5. The excitation wavelength cannot be pushed much redder than 785 nm for Si-based CCD detectors because their sensitivity starts to fall off rapidly at wavelengths past 1,000 nm (see the earlier discussion), which corresponds to Raman shifts (vibrational frequencies) of approximately 3,000 cm^{-1}. The useful "fingerprint" vibrational frequency range necessary to uniquely distinguish most molecular species is 200–2,000 cm^{-1}. The OH and CH stretch frequencies of organic molecules extend past 3,000 cm^{-1}, but it has been found that excluding those regions does not significantly degrade the specificity [23].

Many different methods have been utilized to remove fluorescence baselines from Raman spectra by postprocessing. Schulze et al. [25] have provided an excellent and complete comparison of many of these methods for their consistence, accuracy, reproducibility, performance, computation time, suitability for automation, and modes of failure. They model an experimentally obtained spectrum as the sum of an ideal spectrum **s** and a background **b**, convolved with a blurring function **p**, and with added noise **n**. Then the baseline-correction methods can be divided into methods requiring explicit knowledge of **b**, **p**, or **n** (noise median method [25, 26], first-derivative method [25, 27]), methods requiring explicit estimates of **b** (artificial neural networks [25], threshold-based classification [25, 28], signal removal methods [25], composite (linear-sine-cosine) baseline method [25, 29], spectral shift methods [25, 30–32]), methods requiring explicit use of **b** and **n** (manual methods [25, 33]), methods requiring explicit use of **p**, **b**, and **n** (maximum entropy method [25, 34]), and methods requiring frequency information (Fourier transform method [25, 27], wavelet transform method [25]). Another recent addition is the rolling-circle filter method [35], which we utilize extensively in our own work.

For fluorescence mitigation, diode lasers offer an attractive excitation option. The method of shift-excitation Raman difference spectroscopy (SERDS) has been shown capable of extracting Raman spectra from strong fluorescence interference [30–32]. The method exploits the shift of the Raman spectral features with excitation wavelength, and the (essentially) static or unshifted fluorescence background to distinguish between them. Spectra are obtained using two different but closely spaced excitation wavelengths and then difference or difference-deconvolution methods are used to extract the Raman features. The advantage of diode lasers is that some frequency-stabilization methods can be reprogrammed to produce two or more closely spaced excitation wavelengths, or rapidly shift between them [36], without moving outside the transmission band of the bandpass filter or past the cutoff wavelength of the long wavelength pass filter, allowing SERDS without major retooling. However, to date no commercial portable Raman device offers this option. Recently, multiple-wavelength excitation along with application of an expectation-maximization algorithm was more effective than previous noniterative techniques at extracting Raman features from intense fluorescence with significant shot noise [37].

Another approach to fluorescence mitigation and portability has been recently reported. The approach is based on deep UV excitation, taking advantage of the fact that most explosives (and most other chemical, biological, and explosive materials) fluoresce only beyond approximately 250 nm or longer. For an excitation wavelength of 224.3 nm (transverse-excited hollow-cathode laser [38]), the Stokes Raman spectrum out to 4,000 cm^{-1} ends at 246.4 nm, before the onset of most fluorescence. The photolability of the sample under deep UV excitation will make the method destructive, rather than noninvasive, however. As far as we are aware, any photoreactivity complications during the use of deep UV excitation for Raman detection of explosives have not been reported.

Analyte identification

Once a Raman spectrum has been obtained, the materials being interrogated can be identified; however, the exact methods used by portable Raman instruments to accomplish that task can dramatically affect the accuracy and quality of the results.

To identify a material, a search through a spectral library is usually performed. The search algorithm used is critical

to success, especially for Raman spectra that suffer from interferences, such as fluorescence, thermal emission, or mixtures. In general, the larger the signal-to-noise ratio in the library spectra, the better will be the success of search algorithms. For detection of minor species in a mixture at the 1% level, a signal-to-noise ratio in excess of 300 (RMS noise) is needed (3σ limit of detection criterion), assuming comparable Raman scattering cross sections for the materials. Some portable Raman instruments come with spectral libraries when purchased. For the others, libraries are available at additional cost, or the user must build one. For utilization to identify explosives in the field, we have built our own spectral libraries, as none of the above-mentioned instruments offer a library with a sufficiently large number of explosive materials.

It must be noted that, at the present time, spectral libraries are manufacturer-specific and not transferable. The reasons have to do with abscissa calibration, variation of Raman cross sections with excitation wavelength, ordinate correction for detection system spectral response, and proprietary rather than open-source software and data files. There is progress towards a data standard for Raman spectra, but much work still remains (e.g., ASTM and IUPAC data exchange standard AnIML [39]; see below). For abscissa calibration, the ASTM E-1840 guide recommends several means including standard reference materials with accepted Raman shift wavenumber values [40].

Correction of ordinate data values is more problematic. The ν^4 factor causes changes in Raman signal strength with excitation wavelength. In addition, electronic preresonance and resonance effects can cause changes in the relative intensities of various Raman features depending on their associated chromophore. For a given selected excitation wavelength, however, the ordinate correction process is straightforward. The detected Raman intensities should be multiplied by a relative spectral responsivity correction curve obtained for the entire optical train from sample to detector. Two methods are available to measure the spectral responsivity curve. One method utilizes a calibrated white light irradiance source. More recently, NIST has developed three certified luminous optical glasses (for different excitation wavelengths, 785, 532, and 488/514.5 nm) that emit a broad luminescence spectrum when illuminated with the Raman excitation laser [41]. To perform the correction, either the white light irradiance or the glass luminescence is recorded using the Raman system. Then the spectral irradiance value curve or the relative spectral luminescence curve (I_{SRM}) is used to obtain the spectral intensity correction curve (C_{SRM}) by dividing I_{SRM} by the spectrum measured by the Raman instrument (S_{SRM}). The relative-intensity-corrected Raman spectrum is then obtained by multiplying the measured Raman spectrum by C_{SRM}. However, not all of the commercial portable Raman systems employ ordinate correction.

To achieve spectral data standards that comply with the three stringent criteria for long-term data archiving (readability for long times into the future, robustness to changes in computer hardware and operating systems, and use of public domain data formats), a large number of groups and organizations, including the ASTM subcommittee E13.15 in conjunction with the International Union of Pure and Applied Chemistry (IUPAC), have implemented an Extensible Markup Language (XML) data model, called the Analytical Information Markup Language, or AnIML. The Raman data standard has not yet been completed, but progress can be followed (or assisted) via the Web site [39] and the Web blog set up to track development of software tools to take advantage of the new standard [42].

Explosives-specific issues

For white powder explosives (or other white powders or colorless liquids), portable Raman spectroscopy is a superb method for noninvasive and nondestructive identification. For example, Fig. 4 shows the spectra of octahydro-1,3,5,7-tetranitro-1,3,5,7-tetrazocine (HMX; Holston, beta polymorph) and trinitrotoluene (TNT; recrystallized) obtained using the First Defender in autoaccumulation mode and high laser power (approximately 300 mW). Each spectrum has a signal-to-noise ratio of approximately 100 and took less than 20 s to obtain. The device then correctly identified each material using the spectra in its library.

Even brightly colored yellow, orange, or (some) red composition explosives, such as triaminotrinitrobenzene (TATB) and Semtex 1A and 1H, can be easily identified without safety risks using 785-nm excitation. However, we have found a number of explosive materials that present

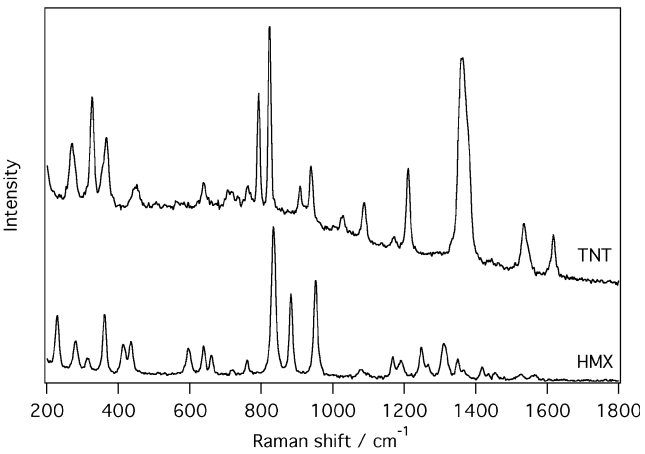

Fig. 4 Raman spectra of trinitrotoluene (*TNT*; recrystallized) and octahydro-1,3,5,7-tetranitro-1,3,5,7-tetrazocine (*HMX*; beta polymorph), obtained using the First Defender, autoaccumulation, high laser power (approximately 300 mW), accumulation time approximately 10-20 s. The TNT spectrum is offset vertically for clarity

some level of signal acquisition difficulty, mostly because of fluorescence, especially in aged materials. These include some compositions and plastic-bonded explosives. Figure 5 shows spectra of flaked TNT and glycidyl azide polymer (GAP), both tan or brownish materials with significant fluorescence, which thereby required significantly longer spectral acquisitions times (several minutes for the flaked TNT to nearly 10 min for the GAP) than for typical white powders to achieve signal-to-noise ratios in excess of 100.

Some explosive materials are dark or highly colored, which can lead to strong absorption of the excitation laser. Harvey et al. [5] have noted the possible safety risks for propellants, military explosives, explosives mixtures, and gunpowders when they are exposed to NIR laser irradiation. They correlated the sample color to the relative ignition risk and showed what distance from their Raman probe was necessary to avoid ignition of the worst materials.

The more important question, however, is whether a Raman spectrum, from which identification can be made, is obtainable for these problematic materials. We found that if one uses very low laser intensities and is willing and able to signal-average for long periods of time, reasonable Raman spectra can be obtained (Fig. 6).

Sample size

Usable Raman spectra can be obtained from white powder sample grains as small as or even smaller than the focal volume of the portable Raman system. As an example, Fig. 7 shows the Raman spectrum from a single sugar grain approximately 100 μm on a side (approximately 60 s exposure, Inspector Raman with NuScope microscope attachment). The total mass of that grain is approximately 1.5 μg. The signal-to-noise ratio in this spectrum is approximately 20. All of the Raman systems in Table 1 have focal sizes 100 μm in diameter or smaller, so it can be claimed that the amount of material needed to obtain a good Raman spectrum using these portable Raman instruments is less than 1 μg. For the example in Fig. 7, the actual focal volume is much less than the grain size owing to the free space optics probe construction (we observed a focus diameter of approximately 10 μm), so the detection limit can be estimated (60-s exposure) to be approximately 2 ng (from $10\times10\times100$ $\mu m^3\times1.5$ $g/cm^3/6.7$, where 6.7 is the signal-to-noise ratio divided by 3; the 3σ criterion) and it was assumed that the depth over which the Raman signal is obtained is limited by the crystal size in that dimension.

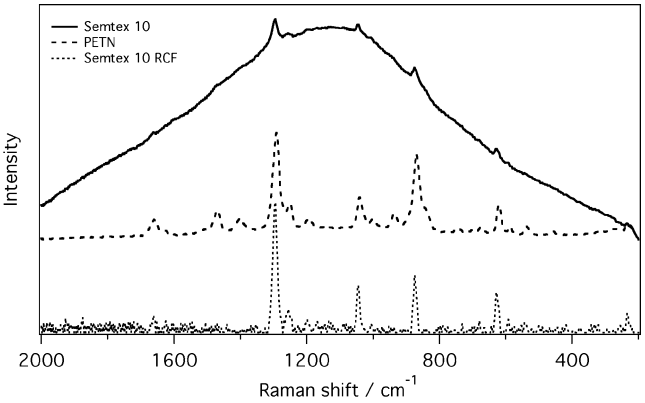

Fig. 6 Raman spectrum of Semtex 10 obtained at 6.5-mW excitation laser power at 785 nm, 60-min total exposure, using the Inspector Raman. Also shown are the Raman spectrum after fluorescence baseline removal (rolling-circle filter, *RCF*) and the reference pentaerythritol tetranitrate (*PETN*) Raman spectrum

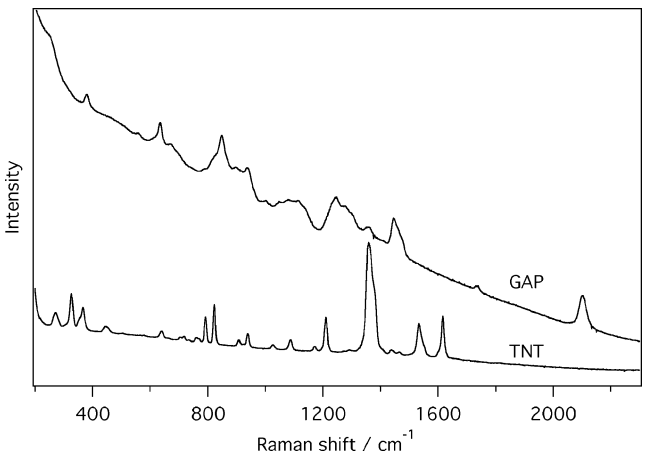

Fig. 5 Raman spectra of slightly colored explosives samples showing the effects of strong fluorescence interference. The TNT is the flaked variety and has a yellowish tan color. The glycidyl azide polymer (*GAP*) is a brownish gel. The advantage of recording spectra to above 2,000 cm^{-1} is clearly illustrated in the GAP spectrum, with the azide stretch visible at 2,102 cm^{-1}. Ordinate zero is the same for both spectra

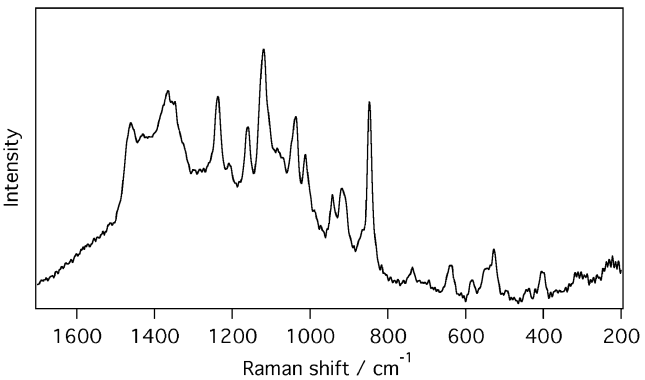

Fig. 7 Raman spectrum from a single sugar grain (C&H Pure Cane Sugar, approximately 100 μm cube, approximately 1.5 μg total mass). Exposure 60 s, 50-mW excitation laser power at 785 nm, using the Inspector Raman with NuScope microscope attachment

Conclusions

There are a number of portable Raman devices available commercially that can identify small amounts of most kinds of explosives in the field. Most are plug powered, but two are self-contained and battery powered. All are capable of obtaining good Raman spectra from white powder explosive samples. However, there are some issues to be solved before Raman spectroscopy is completely suitable for field use: fluorescence and background mitigation, and possible ignition of dark or deeply colored explosives and propellants. Shift-excitation Raman spectroscopy is one possible robust method for fluorescence mitigation. Ignition of some materials remains an issue. The portable Raman devices could be abscissa-calibrated (or did so automatically) using ASTM E-1840 recommendations, but had various degrees of ordinate correction—none using NIST standard reference materials. Explosives spectral libraries are available for some of the portable Raman systems investigated—some are built in, and some must be purchased. A preferred long-term solution will be through the transferability of Raman spectral libraries (long-term data archiving criteria), which is being investigated by ASTM and IUPAC, among others, through the AnIML implementation of the XML data model.

Acknowledgement This work was performed at Los Alamos National Laboratory, operated by Los Alamos National Security, LLC, for the National Nuclear Security Administration of the US Department of Energy under contract DE-AC52-06NA25396.

References

1. Committee on the Review of Existing and Potential Standoff Explosives Detection Techniques, National Research Council (2004) Existing and potential standoff explosives detection techniques. National Academies Press, Washington. http://www.nap.edu/catalog/10998.html
2. Moore DS (2004) Rev Sci Instrum 75:2499–2512
3. Moore DS (2007) Sens Imaging 8:9–18
4. Harvey SD, Vucelick ME, Lee RN, Wright BW (2002) Forensic Sci Int 125:12–21
5. Harvey SD, Peters TJ, Wright BW (2003) Appl Spectrosc 59:580–587
6. Wright CW, Harvey SD, Wright BW (2003) Proc SPIE 5048:107–118
7. Schrader B (1995) Infrared and Raman spectroscopy. VCH, Weinheim
8. Schrader B, Moore DS (1997) Pure Appl Chem 69:1451–1468
9. Weber A (1979) Raman spectroscopy of gases and liquids. Springer, Berlin
10. Long DA (2002) The Raman effect: a unified treatment of the theory of Raman scattering by molecules. Wiley, Chichester
11. Ahura Scientific (2008) http://www.ahurascientific.com/chemical-explosives-id/products/firstdefender/index.php
12. B&W Tek (2006) http://bwtek.com/products/spectrometer_systems/miniature_systems/MiniRamII/MiniRamII.html
13. DeltaNu (2008) http://www.deltanu.com/dn06/products/overview.htm
14. Enwave Optronics (2005) http://www.enwaveopt.com/EZRaman.htm
15. InPhotonics (2007) http://www.inphotonics.com/spectrometers2.htm
16. Ocean Optics (2007) http://www.oceanoptics.com/products/r3000.asp
17. PerkinElmer (2008) http://las.perkinelmer.com/Catalog/ProductInfoPage.htm?ProductID=L1320060
18. Raman Systems (2008) http://www.ramansystems.com/content/view/39/141/
19. Renishaw (2005) http://resources.renishaw.com/en/details/Compact%20Raman%20systems(11218)
20. Senspex (2008) http://www.senspex.com/ramon.html
21. Smiths Detection (2008) http://www.smithsdetection.com/eng/RespondeR_RCI.php
22. Andor Technology (2008) http://www.andor.com/scientific_cameras/idus/models/default.aspx?iProductCodeID=6&tab=tabQECurves. Accessed 17 Sept 2008
23. Lewis IR, Daniel NW Jr., Griffiths PR (1997) Appl Spectrosc 51:1854–1868
24. Lewis ML, Lewis IR, Griffiths PR (2005) Vib Spectrosc 38:17–28
25. Schulze G, Jirasek A, Yu MML, Lim A, Turner RFB, Blades MW (2005) Appl Spectrosc 59:545–574
26. Friedrichs MS (1995) J Biomol NMR 5:147
27. Mosier-Boss PA, Lieberman SH, Newbery R (1995) Appl Spectrosc 49:630
28. Dietrich W, Rudel CH, Neumann M (1991) J Magn Reson 91:1
29. Ruckstuhl AF, Jacobson MP, Field RW, Dodd JA (2001) J Quant Spectrosc Radiat Transf 68:179
30. Shreve AP, Cherepy NJ, Mathies RA (1992) Appl Spectrosc 46:707–711
31. Zhao Z, Carrabba MM, Allen FS (2002) Appl Spectrosc 56:834–845
32. Matousek P, Towrie M, Parker AW (2005) Appl Spectrosc 59:848–851
33. Jirasek A, Schulze G, Yu MML, Blades MW, Turner RFB (2004) Appl Spectrosc 58:1488
34. Phillips AJ, Hamilton PA (1996) Anal Chem 68:4020
35. Brandt NN, Brovko OO, Chikishev AY, Paraschuk OD (2006) Appl Spectrosc 60:288–293
36. Maiwald M, Erbert G, Klehr A, Kronfeldt HD, Schmidt H, Sumpf B, Tränkle G (2006) Appl Phys B 85:509–512
37. McCain ST, Willett RM, Brady DJ (2008) Opt Express 16:10975–10991
38. Hug WF, Reid RD, Bhartia R, Lane AL (2008) Proc SPIE 6954:69540I
39. AnIML: Analytical Information Markup Language (2008) http://animl.sourceforge.net/
40. ASTM International (2002) ASTM E1840-96(2002) Standard guide for Raman shift standards for spectrometer calibration. ASTM International, West Conshohocken
41. Choquette SJ, Etz ES, Hurst WS, Blackburn DH, Leigh SD (2007) Appl. Spectrosc 61:117–129
42. Scimatic Software (2008) http://www.animltools.com/home